Limnological Analysis of North Pipe Lake, Wisconsin: 2019


1 February 2020

1.0 EXECUTIVE SUMMARY.

- North Pipe Lake exhibited strong summer stratification and no evidence of mixing or vertical entrainment and exchanges between the hypolimnion and epilimnion during the summer of 2019, despite the occurrence of a tornado touchdown and potentially high winds in late July. The epilimnetic thickness averaged ~ 3 m.

- The hypolimnion (> 6 m) and metalimnetic depths became anoxic by July 2019. The bottom sediments were anoxic between June and October 2019.

- Laboratory-derived diffusive P flux from sediment under anaerobic conditions was moderate at ~ 4 mg/m^2 d. Soluble phosphorus (P) accumulated in the hypolimnion throughout the summer as a result of this internal P loading mechanism and exceeded 0.40 mg/L above the sediment interface in September 2019.
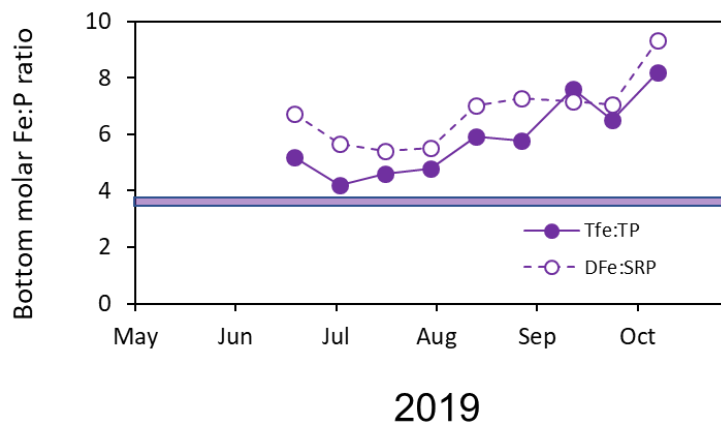
Seasonal variations in the iron:phosphorus ratio in the bottom waters of North Pipe Lake 2019

- Soluble iron also accumulated in the anoxic hypolimnion as a result of a reducing environment and flux from the sediment. The hypolimnetic Fe:P ratio exceeded 4:1, indicating that iron oxyhydroxides (a precipitate that binds with P) forming during reaeration could stoichiometrically bind all the hypolimnetic soluble P and return it back to the sediment. These findings indicated that hypolimnetic soluble P availability for algal uptake during water column mixing periods was likely low and internal P loading was probably not stimulating algal growth in North Pipe Lake.

- Modest chlorophyll blooms developed in the epilimnion in June, early August, and September. Peak chlorophyll was 34 µg/L in September. However, internal P loading was probably not a source for algal uptake, unless these blooms were composed of motile algae that could vertically migrate into the hypolimnion for access to soluble P. Another possible mechanism of direct
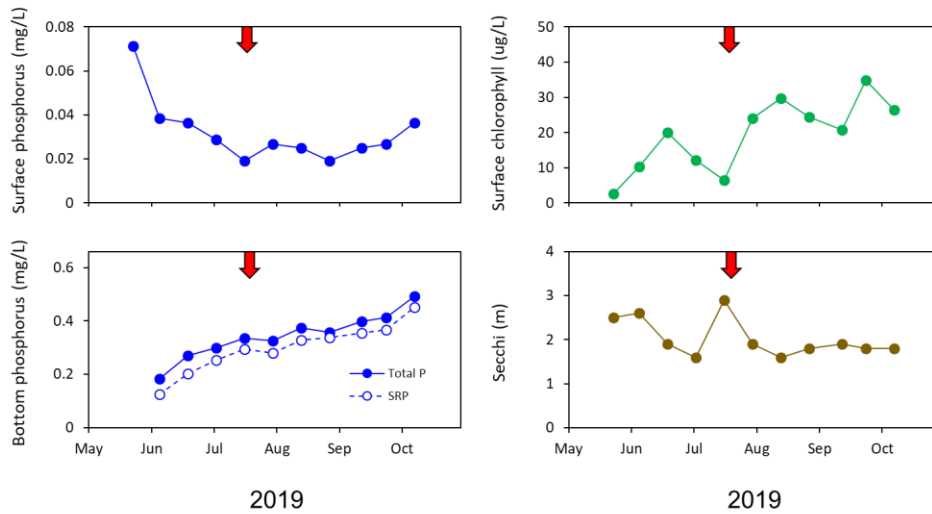
Seasonal variations in surface and bottom phosphorus, chlorophyll, and Secchi transparency in North Pipe Lake 2019

internal P loading access could be from resting spores of akinetes (i.e., cyanobacteria "seeds") residing in the sediment. They may assimilate P directly from the sediment and germinate into the water column under favorable conditions.

- Although alum treatment to control internal P loading is probably not necessary at this time, an initial Al dose of at least 80 g/m^2, split into lower dose applications spread out over multiple years, would be needed. A future maintenance Al dose of 40 g/m^2 should also be factored into the budget to account for Al binding inefficiency due to aging and crystallization. Since North Pipe Lake is poorly buffered, Aluminum sulfate-sodium aluminate should be used to maintain pH at near 7. The recommended treatment area is sediment within the 20-ft contour. This area becomes anoxic throughout the summer. An 80 g/m^2 and 40 g/m^2 treatment would roughly cost $100,000 and $50,000, respectively. However, cost will vary depending on the price of alum at the time of treatment.

2.0 BACKGROUND.

Bottom sediments represent an important internal source of phosphorus (P) that can potentially subsidize high algal productivity, even when external P loading from the watershed has been reduced. For sediments containing iron (Fe) compounds, P can be coupled with Fe recycling and flux to the hypolimnion is regulated by oxidation-reduction reactions (i.e., eH, Mortimer 1971). A thin oxidized microzone exists in the sediment surface layer when the overlying water column is oxygenated. Under these

conditions, Fe is in an oxidized state (i.e., Fe^{+3}) in the microzone as Fe~(OOH) and adsorbs P, thereby controlling its diffusion into the overlying water column. Under anoxic conditions at the sediment-water interface, anaerobic bacterial reduction of iron from Fe^{+3} to Fe^{+2} results in P desorption and diffusion into the hypolimnion. As summer progresses, the slow process of diffusion at the sediment-water interface can lead to the accumulation of considerable soluble PO_4^{3-} and Fe^{2+} in the anoxic hypolimnion.

The availability of this hypolimnetic soluble P to algae residing in the epilimnion is dictated by several factors. Some algae and cyanobacteria can migrate vertically in the water column because they have flagella (a whip-like tail) or can regulate their buoyancy using gas vacuole structures within the cell. For instance, motile algae can migrate downward into the P-rich hypolimnion at night for uptake and then upward into the euphotic zone during the day for photosynthesis. Other nonmotile algae depend on mixing of hypolimnetic P into the epilimnion for uptake. Because density stratification is resistant to disruption and mixing, strong cold fronts, loss of heat from the lake's surface, and sustained winds are usually required for any chance of turbulence and entrainment of hypolimnetic soluble P into the surface waters. Sometimes, P exchange can occur during summer stratification during the passage of cold fronts. Cooling during the autumn leads to complete water column mixing and the potential for entrainment of hypolimnetic P into the surface waters, uptake by algae, and the development of severe blooms.

However, the fate and availability of P after turnover events depends to a large extent on ratio of Fe^{2+} relative to PO_4^{3-} that previously accumulated in the anoxic hypolimnion. When there is sufficient Fe relative to P ("high" Fe:P ratio), most if not all of the PO_4^{3-} becomes coprecipitated or adsorbed to Fe-OOH during reaeration and deposits back to the sediment rather than assimilated by algae. In contrast, when Fe is removed from recycling with PO_4^{3-} in the hypolimnion via reaction with sulfur or organic matter in the sediment, deposition of PO_4^{3-} by Fe-OOH is incomplete, leading to bioavailability for algal uptake during entrainment. Under these circumstances, resulting algal blooms can become extensive and often toxic (i.e., microcystin, etc) as PO_4^{3-} becomes entrained into the surface waters and directly available for uptake and growth. Thus, availability of

hypolimnetic P to algae needs to be considered in management approaches to internal P loading.

3.0 OBJECTIVES.

The objectives of these investigations are several-fold:

1. Detail the development of thermal stratification and mixing using thermistors (i.e., temperature data loggers) deployed in the lake at ~1-m intervals to document stratification and mixing patterns that might lead to P entrainment from the hypolimnion into the epilimnion,

2. examine vertical profiles of temperature, dissolved oxygen, chlorophyll, iron (Fe), and P to determine the buildup of hypolimnetic Fe and P, the hypolimnetic Fe:P ratio, the potential for incomplete P control by Fe, and linkages to algal bloom development. Monitor vertical variations in chlorophyll during the summer stratified period and Fall turnover in an effort to link mixing and entrainment events to algal bloom development or vertical migration potential,

3. measure rates of P release from sediment under anaerobic conditions from intact sediment cores to estimate internal P loading potential from hypolimnetic sediment,

4. examine vertical variations in sediment mobile P fractions in sediment cores that are active in internal P loading for estimation of alum dosage and quantify the thickness of the mobile P layer in the sediment (i.e., active sediment layer contributing to internal P loading) that needs to be controlled by alum,

5. estimate the dosage of alum (as aluminum or Al) required to bind mobile P fractions in this active sediment layer and provide cost estimates for Al application based on treatment areas in the lake.

4.0 METHODS.

Stratification and mixing dynamics in North Pipe Lake

Data logging thermistors (HOBO temperature loggers, Onset, Corp) were deployed in the deepest region of the lake (Fig. 1) at 1-m intervals from the surface to near bottom to record temperature at 1-hour intervals between June and October 2019, in order to quantify the frequency of occurrence of stratification and mixing periods. The thermistor string was moved to shore apparently by vandals in mid-July. We moved it back into position in late July but there was a period of ~ 2 weeks of lost data (14 to 21 July 2019).

Schmidt stability (S; g-cm/cm^2) was calculated as:

$$S = 1/A \int_0^{z_m} (z - z_g)(\rho_z - \rho_g)dz$$

where A = surface area (m^2), z_m = maximum depth (m), z = depth at stratum z, z_g = depth of the center of mass or ρ_g, and ρ_z = the density of water (kg/m^3) at depth z (Idso 1973). ρ_g was calculated as:

$$\rho_g = 1/V \int_0^{z_m} V_z \rho_z dz$$

where V is lake volume (m^3) and V_z is the volume at depth z. Schmidt stability represented the amount of work (in the form of wind power, motor boat activity, etc) required to completely mix a water body (without loss of gain in heat content) that is stratified due to vertical differences in water density. Higher stability values were indicative of strong stratification and greater work required to disrupt stratification. Conversely, lower stability values were indicative of weak stratification and less work required to disrupt stratification. The location of the metalimnion was quantified using

6

the Relative Thermal Resistance to Mixing (RTRM) statistic (Vallentyne 1957). An RTRM of 30 was used to define the location of the metalimnion.

Seasonal and vertical variations in water chemistry

Water samples for limnological variables were collected biweekly between late May and early October at the same station in the deepest portion of the lake (Fig. 1 and Table 1). An integrated sample was collected over the upper 2-m for analysis of total phosphorus and chlorophyll a. Discrete samples were collected at 1-m

Table 1. Station locations in North Pipe Lake.			
Station	East (Dec Deg)	North (Dec Deg)	Depth (m)
NPL North	45.53429	-92.2002	9.9
NPL Central	45.53237	-92.1993	10.9
NPL South	45.53054	-92.1997	8

intervals from the lake surface to near the bottom for total and soluble reactive P and chlorophyll analysis using a peristaltic pump and Tygon® tubing (3/16 inch inner diameter). A portion of the bottom water sample was sent to the Wisconsin State Laboratory of Hygiene for analysis of total and dissolved Fe. Secchi transparency and in situ measurements (temperature, dissolved oxygen, pH, and conductivity) were collected on each date. In situ measurements were recorded at 1-m intervals using a YSI 6600 data sonde (Yellow Springs Instruments, Inc., Yellow Springs, OH) that was precalibrated with known pH buffers and independent Winkler titrations for dissolved oxygen (APHA 2011).

Samples for total P were digested with potassium persulfate prior to analysis (APHA 2011). Samples for soluble reactive P were filtered immediately in the field using a 0.45 µm pore size syringe filter. Phosphorus was analyzed on a Perkin-Elmer UV-VIS Lambda 25 Spectrophotometer using the ascorbic acid method (APHA 2011). Samples for chlorophyll analysis were filtered onto a type A/E glass fiber filter, extracted in 90% acetone overnight in the freezer, and analyzed fluorometrically using a TD 300 fluorometer (Turner Designs).

Laboratory-derived diffusive phosphorus flux from sediment under anaerobic conditions

Replicate intact sediment cores were collected from the station located in the deepest portion of the lake for the determination of diffusive P flux from sediment under controlled laboratory conditions (Fig. 1). Cores were carefully drained of overlying water in the laboratory and the upper 10 cm of sediment were transferred intact to a smaller acrylic core liner (6.5-cm dia and 20-cm ht) using a core remover tool. Surface water collected from each lake was filtered through a glass fiber filter (Gelman A-E), with 300 mL then siphoned onto the sediment contained in the small acrylic core liner without causing sediment resuspension. They were placed in a darkened environmental chamber and incubated at a constant temperature of ~10 $^{\circ}$C to reflect summer hypolimnetic water temperature conditions. The Eh environment in the overlying water was controlled by gently bubbling nitrogen-CO_2 (anaerobic) through an air stone placed just above the sediment surface in each system. Bubbling action insured complete mixing of the water column but not disrupt the sediment.

Water samples for soluble reactive P were collected from the center of each system using an acid-washed syringe and filtered through a 0.45 µm membrane syringe filter. The water volume removed from each system during sampling was replaced by addition of filtered lake water preadjusted to the proper oxidation-reduction condition. These volumes were accurately measured for determination of dilution effects. Soluble reactive P was measured colorimetrically using the ascorbic acid method (APHA 2011). Rates of P release from the sediment (mg/m^2 d) were calculated as the linear change in mass in the overlying water divided by time (days) and the area (m^2) of the incubation core liner. Regression analysis was used to estimate rates over the linear portion of the data.

Spatial and vertical evaluation of sediment P characteristics

The objectives of this task were to quantify spatial and vertical variations in sediment P fractions in different areas of North Pipe Lake for use in examining mobile P pools and estimating the thickness of the sediment layer that needs to be treated with aluminum

sulfate. The thickness of the upper sediment layer that is potentially active in internal P loading was determined by evaluating vertical P profiles according to Carey and Rydin (2011). Typically, sediment P concentrations are elevated in the upper layer versus deeper layers of eutrophic lake sediments due to accumulation of mobile sediment P in excess of burial and breakdown. For the deep basin station (i.e., central station), a sediment core was sectioned at 1-cm intervals over the upper 6 cm, 2-cm intervals down to 10 cm, and 2.5-cm intervals to 15 cm for analysis of sediment P fractions. The upper 5-cm was sectioned at 2 additional shallower stations (i.e., north and south stations) located within the anoxic hypolimnetic area for sediment chemistry. Sediment sections were analyzed for moisture content, sediment density, organic matter content, loosely-bound P, iron-bound P, labile organic P, and aluminum-bound P. Subsamples were dried at 105 °C to a constant weight and burned at 550 °C for determination of moisture content, sediment density, and organic matter content (Håkanson and Jensson 2002). Phosphorus fractionation was conducted according to Hieltjes and Lijklema (1980), Psenner and Puckso (1988), and Nürnberg (1988) for the determination of ammonium-chloride-extractable P (1 M NH_4Cl; loosely-bound P), bicarbonate-dithionite-extractable P (0.11 M BD; iron-bound P), and sodium hydroxide-extractable P (0.1 N NaOH; aluminum-bound P). A subsample of the sodium hydroxide extract was digested with potassium persulfate to determine nonreactive sodium hydroxide-extractable P (Psenner and Puckso 1988). Labile organic P was calculated as the difference between reactive and nonreactive sodium hydroxide-extractable P.

The loosely-bound and iron-bound P fractions are readily mobilized at the sediment-water interface under anaerobic conditions that result in desorption of P from bacterially-reduced iron compounds (i.e., Fe^{+3} to Fe^{+2}) in the sediment and diffusion into the overlying water column (Mortimer 1971, Boström 1984, Nürnberg 1988). The sum of the loosely-bound and iron-bound P fractions are referred to as redox-sensitive P (i.e., redox-P; the P fraction that is active in P release under anaerobic and reducing conditions). In addition, labile organic P can be converted to soluble P more slowly via bacterial mineralization (Jensen and Andersen 1992) or hydrolysis of bacterial polyphosphates to soluble phosphate under anaerobic conditions (Gächter et al. 1988; Gächter and Meyer

9

1993; Hupfer et al. 1995). The sum of redox-P and labile organic P is collectively referred to a biologically-labile P. This fraction is generally active in recycling pathways that result in exchanges of phosphate from the sediment to the overlying water column and potential assimilation by algae.

Alum dosage determination

Al dosage was estimated as the concentration (g/m^2) required to bind redox-P. This dry mass P concentration (mg/g) was converted to an area-based concentration (g/m^2) as,

$$P \ (g/m^2) = P \ (mg/g) \cdot \rho \ (g/cm^3) \cdot \theta \cdot h \ (m) \cdot 1000000 \ (cm^3/m^3) \cdot 0.001 \ (g/mg)$$

where, ρ is sediment bulk density (g/cm^3), θ is sediment porosity (100 – percent moisture content; dimensionless), and h is sediment thickness (m). The Al concentration (g/m^2) was estimated as,

$$Al \ (g/m^2) = P \ (g/m^2) \cdot Al{:}P$$

where, Al:P is the binding ratio estimated from James and Bischoff (2015).

The application area was estimated based on the extent and timing of summer hypolimnetic anoxia in North Pipe Lake. The application strategy is based on recent publications by Lewandowski et al. (2003), de Vicente et al (2008a and b), Jensen et al. (2015), and Huser et al. (2016).

A titration procedure was used to determine the maximum allowable dosage of alum to maintain pH above 6.0. The hydrolysis of Al leads to the production of hydrogen ions which lowers the pH of the water column. Al toxicity to the biota can occur if the pH falls below 6 and must be considered in dose determination. Lake water was titrated with alum to determine this maximum allowable dosage and compared with the dosage based on sediment redox-P. For situations where alkalinity is low or the required dosage

exceeds maximum allowable dosage, buffered aluminum sulfate-sodium aluminate treatment will be needed to maintain pH above 6.0.

5.0 RESULTS.

Limnological conditions

Annual precipitation measured at Amery WI was above normal in 2019 compared to the average since 1980 (Fig. 2). Local precipitation (also measured at Amery WI) in excess of 1 inch occurred in mid- and late July, early and mid-August, and late September (Fig. 3). In addition, severe storms, high winds, and tornado touchdowns occurred in the vicinity on 19 July, resulting in local precipitation in excess of 2 inches (Fig. 3).

The thermistor string deployed in the deep basin of North Pipe Lake captured strongly stratified conditions throughout June into early October (Fig. 4). Schmidt stability (the work required to completely mix the lake without loss of heat) was very high throughout this period. The epilimnion was ~ 2 m thick in July and expanded to 4 m in September as a result of gradual heat loss and epilimnetic expansion during the approach of Autumnal turnover. The metalimnion was > 2 m thick and characterized by steep temperature-density gradients throughout the summer (Fig. 4). There was some downward heat transfer to the upper hypolimnion between August and early September as suggested by gradual increases in temperature at the 7- and 8-m depths. This pattern coincided with epilimnetic expansion. However, bottom temperature (> 9 m) increased only slightly throughout the summer and generally remained below ~ 7 C suggesting negligible mixing or entrainment from deep density layers in the lake. A period of cooling in late September resulted in substantial epilimnetic expansion down to the 5-m depth. Epilimnetic expansion and Autumnal turnover started in late September but was not complete by the end of the study in mid-October.

Fluctuations in Schmidt stability, heat content, and mean lake temperature coincided with the passage of cold and warm fronts (Fig. 5). Heat loss and mean lake temperature declines occurred in early June followed by ~ linear net gains in heat and increases in mean lake temperature until early August (Fig. 5). Severe storms and tornado touchdowns occurred on 19 July after the thermistor string was vandalized. Trends in vertical temperature profiles after this storm period suggested some mixing and slight epilimnetic expansion occurred in conjunction with decreased Schmidt stability (Fig. 4). However, disruption of the metalimnion and potential entrainment of water located in the upper hypolimnion was probably minor. Heat loss from the lake and declines in mean lake temperature between August and September coincided with decreased Schmidt stability. However, stratification remained strong during this period and vertical entrainment of water and nutrients (P) into the epilimnion was negligible.

Bottom anoxia had become established in June 2019 and rapidly extended to the 4-m depth, within the metalimnion, in early July (Fig. 6). Anoxic conditions occurred between the lake bottom and ~4 m through mid-August. The vertical depth of anoxia declined to ~ 5 m in early September in conjunction with epilimnion expansion and metalimnetic downward migration. Mixing and the onset of Autumnal turnover in October resulted in reaeration of the upper 8 m water column. However, bottom anoxia continued into mid-October. Overall, bottom anoxia and reducing conditions for diffusive P flux from sediment under anaerobic conditions persisted throughout the research period.

Iron and P increased approximately linearly above the sediment-water interface throughout the summer stratified period in conjunction with bottom anoxia (Fig. 7). This pattern can be attributed to anaerobic bacterial reduction of iron oxyhydroxide ($Fe^{3+}(OOH)$ to Fe^{2+}), desorption of PO_4-P and diffusive flux of both Fe^{2+} and PO_4-P into the hypolimnion (Mortimer 1971). In addition, the molar Fe:P ratio exceeded 3.6:1 in the bottom waters (Fig. 8), suggesting that there was enough Fe to bind all PO_4-P and remove it back to the sediment during reaeration of the hypolimnion and chemical oxidation to $Fe^{3+}(OOH)$. Thus, Fe oxidation serves to bind PO_4-P and remove most of it from

potential uptake by algae during periods of mixing and vertical entrainment in North Pipe Lake.

In other lakes, Fe^{2+} can react with sulfur (S) in the sediment to form FeS which is an inert mineral that becomes removed from further reaction and interaction with PO_4-P (Caraco et al. 1991, 1993, Kleeberg 1997, Golterman 2001). Generally, these lakes exhibit high sulfate input relative to iron. Dissolved organic matter (DOC) can also sequester Fe^{2+} and remove it from further reactivity with PO_4-P (Kleeberg et al. 2012, 2013; LaLonde et al. 2013). In the case of North Pipe Lake, iron appears to be largely trapping PO_4-P in the hypolimnion and sediment. In lakes where hypolimnetic iron is not in stoichiometric supply relative to PO_4-P (i.e., < 3.6:1 molar) due to reaction with S or DOC, PO_4-P can become entrained into the epilimnion for direct assimilation by algae (James et al. 2017).

P accumulated in the hypolimnion as a result of internal P loading and concentrations were relatively high above the sediment-water interface by the end of September at > 0.350 mg/L (total P and SRP, Fig. 9 and Table 2). P concentration gradients also extended into the base of the metalimnion in August and September. However, iron likely sequestered and redeposited most of this P via chemical oxidation during periods of epilimnetic expansion and downward metalimnetic migration due to a high Fe:P ratio.

Table 2. Ssummer (Jun-Sep) lake limnological variable means for North Pipe Lake in 2019. P = phosphorus, TSI = trophic state index, CHLa = chlorophyll.

	Mean	Median	Min	Max
Surface Total P (mg/L)	0.027	0.027	0.019	0.038
Bottom Total P (mg/L)	0.329	0.336	0.183	0.413
Bottom soluble reactive P (mg/L)	0.283	0.295	0.126	0.367
Chlorophyll (ug/L)	20.27	20.68	6.48	34.8
Secchi transparency (m)	2	1.9	1.6	2.9
Secchi transparency (ft)	6.6	6.2	5.2	9.5
Carlson TSI-TP	52	52	47	57
Carlson TSI-CHLa	59	60	49	65
Carlson TSI-SD	50	51	45	53
WI TSI-TP	54	54	51	56
WI TSI-CHLa	57	58	59	62
WI TSI-SD	50	51	45	53

Seasonally, the surface total P concentration was relatively high in late May; however, the chlorophyll concentration was low (Fig. 10). This pattern may have been the result of

zooplankton grazing (i.e., clearing period where zooplankton graze mostly edible phytoplankton such as green algae and diatoms), which commonly occurs during the late Spring period. Grazing of algae can result in incorporation of P into zooplankton biomass, leading to low chlorophyll but high total P concentrations as zooplankton biomass. Other factors leading to high total P include carryover of internal P loadings (as total P) and mixing into the water column after iceout and loading of particulate P from the watershed during Spring storm events.

Modest peaks in surface (i.e., upper 2-m integrated) chlorophyll occurred during the summer stratified period in early June, early August, and mid-September (Fig. 10). Peak chlorophyll in early August and September coincided with the tornadic storms (19 July) and precipitation periods (September). The late September surface chlorophyll peak also coincided with other environmental factors. Water column cooling, mixing and epilimnetic expansion occurred prior to the late September chlorophyll peak (Fig. 5), which might have favored diatom bloom formation. Diatoms typically bloom during Spring and Autumnal turnover periods.

Interestingly, chlorophyll concentrations also increased at the base of the metalimnion (~ 6 m) in late summer at the oxycline where dissolved oxygen concentrations approached zero (Fig. 9). The algal assemblage and major genera comprising this bloom are unknown. Metalimnetic bloom formation started in late August and exhibited peak concentrations (> 60 µg/L) in late September. The bloom also had access to hypolimnetic P gradients that originated from internal P loading. Coincidently, chlorophyll concentrations increased to ~ 35 µg/L in the surface waters in late September (Fig. 9). However, these chlorophyll maxima were vertically separated by several meters and most likely not connected. Usually, migrating algae like certain cyanobacteria (*Microcystis*, *Aphanizomenon*) and dinoflagellates (*Ceratium*) exhibit surface peaks during the day and migrate downward at night (Taylor et al. 1988, James et al. 1992, Gervais et al. 2003). Other algal genera may selectively reside in the metalimnion at low light and dissolved oxygen levels where grazing pressure is minor (Gervais et al. 2003). More information is

14

needed such as algal genera identification to better understand seasonal and vertical distribution and dynamics of the algal assemblage in North Pipe Lake.

Relationships between total P and chlorophyll in the epilimnion were weak and statistically not significant (Fig. 11). The extreme outlier (denoted with red circle in Fig. 11) was collected in late May. As discussed earlier, this very low CHLa:TP ratio may have been due to zooplankton grazing. For other dates, chlorophyll fluctuated between 6 µg/L and 35 µg/L over a relatively constant mean of 0.028 mg/L total P (range = 0.019 mg/L to 0.038 mg/L) and chlorophyll TSI (Trophic State Index) tended to be proportionately high relative to total P and Secchi transparency, particularly between late July and early October (Fig. 12). Finally, the ratio between chlorophyll and total P (CHLa:TP ratio) changed throughout the summer (Fig. 13). It was lower in June to early July and increased in August through September. This pattern may have been related to seasonal succession from diatoms and green algae to cyanobacteria but more information is needed to better understand relationships algae and nutrients in North Pipe Lake.

Summer means (Jun-Sep) for various limnological variables are listed in Table 2. Overall, summer mean surface total P, chlorophyll, and Secchi transparency were 0.027 mg/L, 20.3 µg/L, and 2 m (6.6 ft), respectively. North Pipe Lake was moderately eutrophic. Carlson TSI ranged between 50 and 59 while Wisconsin TSI ranged between 50 and 57.

Diffusive phosphorus flux and sediment characteristics

Table 3. Laboratory-derived anaerobic diffusive phosphorus flux from sediments collected in North Pipe Lake. SE = 1 standard error.	
Variable	$(mg/m^2\ d)$
Rep 1	5.03
Rep 2	3.01
Rep 3	4.05
Mean	4.03
SE	0.58

Soluble phosphorus concentration increased linearly in the overlying water column with respect to days of incubation under anaerobic (i.e., no dissolved oxygen) conditions (Fig. 14). The mean anaerobic diffusive P flux measured at the deep basin station in North Pipe Lake at ~ 10 C was moderate at ~ 4 mg/m^2 d (Table 3) and fell near the median compared to other lakes in the region (Fig. 15).

Sediment moisture content exceeded 95% and wet bulk density approached 1 g/cm^3 (i.e., density of water at 4 C) in the upper 2-cm sediment layer, suggesting very flocculent sediment (Fig. 16). Organic matter content was also high in the upper 2-cm sediment layer at ~ 38%. This pattern may be attributable to algal and perhaps macrophyte remains concentrated near the sediment surface.

Biologically-labile (i.e., subject to recycling pathways leading to internal P loading) P concentrations exhibited a very modest peak in the upper 2-cm layer and declined to lower concentrations below the 6-cm sediment depth (Fig. 16f). Surface concentration bulges can reflect the buildup of potentially mobile P in excess of burial, a pattern typically observed in eutrophic lake systems exhibiting internal P loading and low P burial efficiency (Carey and Rydin 2011, Rydin et al. 2011). However, surface versus subsurface biologically-labile P concentration differences were very modest to minor for North Pipe Lake sediments, suggesting relatively efficient P burial. The surface biologically-labile P concentration was 1.383 mg/g and the concentration declined between the 65- and 10-cm sediment depth to ~ 0.924 mg/g.

Labile organic P was the dominant biologically-labile fraction in the upper 5-cm sediment layer at 53% to 74% (Fig. 17). The concentration was also high relative to sediment cores collected in other lakes in the region (Fig. 18). Iron-bound P was the next dominant fraction, accounting for 21 to 42% of the biologically labile P. The iron-bound

P concentration was relatively high in North Pipe Lake and fell within the upper 25% quartile compared to other lakes (Fig. 18). Overall, redox-P concentrations (i.e., the sum of loosely-bound and iron-bound P) in the upper 5-cm sediment layer of North Pipe Lake fell within the upper 25% quartile and biologically-labile P fell above the upper 25% quartile, primarily due to high labile organic P concentrations (Fig. 19).

Summer phosphorus mass balance and budget

To examine seasonal changes in total P mass and mean concentration in North Pipe Lake, I assumed the mean epilimnetic depth and thickness over the summer period was 3 m. Mean epilimnetic P concentration was maximal in late May-early June at 0.067 mg/L and declined steadily to 0.034 mg/L in early July due most likely to net sedimentation of algal cells (Fig. 20). The mean epilimnetic concentration fluctuated between 0.034 mg/L and 0.039 mg/L from mid-July to late September, then increased to 0.052 mg/L in early October as the lake started turning over and entraining hypolimnetic water enriched with P from internal loads. The increase in mean epilimnetic P in late July through early August coincided with increases in chlorophyll, suggesting incorporation of P into cellular algal biomass during growth. This pattern occurred shortly after the tornadic storm (19 July) suggesting that watershed P loading might have been the likely source of this P (and chlorophyll) increase. Vertical entrainment of hypolimnetic P was probably minor because lake water column stability was relatively high with strongly stratified condition during this period.

Hypolimnetic (i.e. depths > 3 m) P concentrations and mass increased approximately linearly between early June and October as a result of anaerobic diffusive P flux from sediment and accumulation in the hypolimnion (Fig. 20). The anoxic factor (i.e., "number of days that a sediment area equal to the lake surface area is overlain by anoxic water", Nürnberg 1995) was ~ 68 d.

Table 4. Estimates of summer net internal phosphorus (P) loading (as kg/summer or kg/y) in North Pipe Lake.

Estimation method	Net internal P load (kg)	Source
Hypolimnetic P accumulation	55	This research
Anaerobic diffusive P flux	68	This research
Method 1 - total P budget	-1 to 3	Pipe and North Pipe Lakes Lake Management Plan, 2018-2023
Method 2 - in situ P increases	76 to 185	Pipe and North Pipe Lakes Lake Management Plan, 2018-2023
Method 3 - in situ fall increases	-3 to 137	Pipe and North Pipe Lakes Lake Management Plan, 2018-2023
Method 4 - P release x anoxic area	64	Pipe and North Pipe Lakes Lake Management Plan, 2018-2023

Internal P loading during the summer was estimated using 2 approaches to obtain ranges: 1) changes in hypolimnetic P mass accumulation and 2) laboratory-derived diffusive P fluxes multiplied by anoxic factor. The change in hypolimnetic P mass between early June and late September (112 d) was 55 kg (Table 4). Contributions from diffusive P flux over the same time period were estimated at 68 kg (Table 4). The discrepancy between the two estimates can be attributed to net sedimentation. Hypolimnetic P mass accumulation reflects net internal P loading because it includes net P sedimentation. Laboratory diffusive P flux $\times$ anoxic area represents gross internal P loading because this calculation does not include net P sedimentation from the water column. Estimates of internal P loading from this study generally fell within ranges estimated using other methods (Polk County, Table 4).

Alum dose estimation and application area

Al dose and application area - Alum dosage was based on redox P concentrations in the upper 6-cm sediment layer (Table 5 and Fig. 16). Redox P concentrations were slightly higher in this region of the sediment column compared to concentrations between > 6- and 10-cm and, thus, represented potential internal P loading in excess of P burial. The Al:P ratio required to bind this redox P was estimated from James and Bischoff (2015) for sediment collected in the north, central, and south regions of the deep basin. The Al dose averaged 80 g/m^2 and ranged between 76 and 83 g/m^2 (Table 5). This concentration is lower than those estimated for some other lakes in the region primarily because sediment redox P is lower in North Pipe Lake (Table 6).

Table 5. Estimated aluminum (Al) dose to inactivate redox phosphorus (i.e., loosely-bound plus iron-bound P in the sediment) in the upper 6-cm sediment layer. The Al:P binding ratio was calculated from regression relationshipos presented in James and Bischoff (2015).

Station	Mean Redox-P		Estimated Al:P ratio	Estimated Al Dose
	(mg/g)	(g/m^2)		(g/m^2)
North	0.329	1.341	62	83
Central	0.520	1.657	46	76
South	0.534	1.803	45	82
Average				80

Because total alkalinity is very low in North Pipe Lake (~ 10 mg/L), alum applications will need to be buffered to regulate pH. Al binding of P is most efficient within a pH range of 6 to 8. As pH declines below 6, Al becomes increasingly soluble (as Al^{3+}) and toxic to biota. The maximum allowable Al dosage that could be applied and yet maintain pH at or above 6, determined via jar tests (Cooke et al. 2005), was very low at 1.25 mg Al/L. Al dosage up to 80 g/m^2 would fall well above the maximum allowable dosage, indicating that aluminum sulfate could not be safely applied without decreasing the pH to < 6.

Table 6. Recent alum (as Al) dosages for various lakes.		
Lake	Al Dose (g Al/m^2)	Reference
North Pipe Lake, WI	80	Present study
East Balsam Lake	100	(James unpubl. data)
Long Lake, WI	105	(James unpubl. data)
Cedar Lake, WI	100-130	(James unpubl. data)
Lake Riley, MN	100	(James unpubl. data)
Bald Eagle, MN	100	(James unpubl. data)
Black Hawk, MN	145	(James unpubl. data)
Tiefwarensee, Germany	137	Wauer et al. (2009)
East Alaska, WI	132	Hoyman (2012)
Half Moon, WI	75-150	James (2011)
Susser See, Germany	100	Lewandowski et al. (2003)
Green, WA	94	Dugopolski et al. (2008)

The suggested application area is sediment located below the 20-ft contour. This sediment area is located within the hypolimnion, becomes anoxic throughout the summer (Fig. 6), and contains anoxic sediment that contributes to internal P loading. This area was estimated at ~ 28.5 acres using digitizing software (Didger 5, Golden Software, Golden CO) and bathymetric map obtained from Lake-Link (https://www.lake-link.com/wisconsin-lakes/polk-county/pipe-lake-north/3707/).

Al application strategy and ~ cost- Because the Al floc can polymerize significantly if not immediately exposed to P and lose binding sites (De Vicinte et al. 2008a), it is important for the Lakes District to consider splitting the dose and applying alum over

Table 7. An example adaptive management scenerio approach in which the Al dose is split into smaller applications. A smaller dose is applied to lake sediments in year 1. The second Al application and dose is determined via annual sediment profile monitoring. In this example, annual sediment core vertical profiling indicated that a second application should occur in year 3 at a dose estimated from similar core analysis.

Variable	Year 1	Year 2	Year 3	Year 4	Year 5	Year 4	Year 5
Al application	40 g/m^2		25 g/m^2		15 g/m^2		15 g/m^2
Assessment[1]							

[1]Sediment core collection and vertical profile monitoring

multiple years to improve binding efficiency and longevity of internal P loading control (Table 7). A future maintenance treatment should also be incorporated into the management plan for budgeting purposes.

Other research (de Vicente et al 2008, Huser 2012, James 2017b) has suggested development of an adaptive management approach of applying Al concentrations spread out over a period of years (i.e., 1-3-year intervals) and monitoring lake response for future Al maintenance applications. In addition, application of alum during later summer when hypolimnetic P concentrations are relatively high (late August-September) would enhance exposure of the settling Al floc to P, promote immediate binding of a portion of the internal P load, and improve long-term binding capacity and efficiency. Application of multiple Al concentrations spread out over a period of years may be more effective in saturating binding sites, lowering the Al:P binding ratio, and stabilizing polymerization for longer internal P loading control. Dose splitting can also be used as an adaptive management approach to address slower degradation of labile organic P into mobile forms as well as increased P binding efficiency onto the Al floc.

The cost of an 80 g/m^2 buffered alum treatment is projected at ~ $100,000 for planning purposes. An exact and accurate cost for split dose applications would need to be obtained during the year of treatment because alum costs fluctuate on the market. A future maintenance Al dose of 40 g/m^2 would roughly cost ~ $40,000. This maintenance strategy could also be split into lower doses spread out over multiple years.

Table 8 Projected costs for various Al doses to sediment below the 20-ft depth contour.

	80	40
Buffered Al dose (g/m^2)	80	40
Treatment area (acres)	28.487	28.487
Aluminum sulfate (gal)	18,096	9,048
Sodium aluminate (gal)	9,048	4,524
~ Cost ($)[1]	$100,000	$50,000

[1]Actual cost may vary depending on the market caalue of buffered alum at the time of treatment

4.0 CONCLUSIONS AND RECOMMENDATIONS

Although internal P loading is moderate and hypolimnetic P concentrations increase in excess of 0.35 mg/L near the sediment-water interface during the summer, iron appears to be trapping this P back to the sediment, minimizing its availability to the epilimnion. Based on the high hypolimnetic Fe:P ratio, the availability of internal P loads to the epilimnion via mixing and vertical entrainment are very low. Thus, the primary mode of access to hypolimnetic P gradients would be through vertical migration by cyanobacteria, *Ceratium hirundinella,* or other algae residing in the lower metalimnion or upper hypolimnion. Unless vertically-migrating algal species are taking advantage of hypolimnetic P gradients, Al treatment is not necessary for North Pipe Lake.

More information could be collected to better understand seasonal algal bloom dynamics. Recommendations include a better understanding of algal genera percentage of the assemblage that are cyanobacteria, and the potential for vertical motility in the lake. Finally, many cyanobacteria can form resting stages as akinetes or spores that reside in the sediment and germinate under optimal environmental conditions. These resting stages may directly assimilate sediment P in excess of growth requirements and develop blooms when inoculating the water column (Istvanovics et al. 1993, 2000; Pettersson et al. 1993; Perakis et al. 1996; Cottingham et al. 2015). More information is needed on the algal species assemblage to verify the possibility of akinete-forming cyanobacteria.

5.0 REFERENCES.

APHA (American Public Health Association). 2011. Standard Methods for the Examination of Water and Wastewater. 22th ed. American Public Health Association, American Water Works Association, Water Environment Federation.

Boström B. 1984. Potential mobility of phosphorus in different types of lake sediments. Int Revue Ges Hydrobiol 69:457-474.

Caraco N, Cole JJ, Likens GE. 1991. A cross-system study of phosphorus release from lake sediments. In: Cole J, Lovett G, Findlay S, editors. Comparative analyses of ecosystems: Patterns, mechanisms, and Theories. Springer-Verlag, NY.

Caraco NF, Cole JJ, Likens GE. 1993. Sulfate control of phosphorus availability in lakes. Hydrobiologia 253:275-280.

Carey C, Rydin E. 2011. Lake trophic status can be determined by the depth distribution of sediment phosphorus. Limnol Oceanogr 56:2051-2063.

Cooke GD, Welch EB, Peterson SA, Nichols SA. 2005. Restoration and management of lakes and reservoirs. 3rd ed. Boca Raton (FL): CRC Press.

Cottingham KL, Ewing HA, Greer ML, Carey CC, Weathers KC. 2015. Cyanobacteria as biological drivers of lake nitrogen and phosphorus cycling. Ecosphere. 6:1–19.

de Vicente I, Huang P, Andersen FØ, Jensen HS. 2008a. Phosphate adsorption by fresh and aged aluminum hydroxide. Consequences for lake restoration. Environ Sci Technol 42:6650-6655.

de Vicente I, Jensen HS, Andersen FØ. 2008b. Factors affecting phosphate adsorption to aluminum in lake water: Implications for lake restoration. Sci Total Environ 389:29-36.

Gächter R., Meyer JS, Mares A. 1988. Contribution of bacteria to release and fixation of phosphorus in lake sediments. Limnol Oceanogr 33:1542-1558.

Gächter R, Meyer JS. 1993. The role of microorganisms in mobilization and fixation of phosphorus in sediments. Hydrobiologia 253:103-121.

Gervais F. Siedal U, Heilmann B, Weithoff G, Heisig-Gunkel G, Nicklisch A. 2003. Small-scale vertical distribution of phytoplankton, nutrients and sulphide below the oxycline of a mesoeutrophic lake. J Plank Res 25:273-278.

Golterman HL. 2001. Phosphate release from anoxic sediments or 'what did Mortimer really write? Hydrobiologia 450:99-106.

Gunnars A, Blomqvist S, Johansson P, Anderson C. 2002. Formation of Fe(III) oxyhydroxide colloids in freshwater and brackish seawater, with incorporation of phosphate and calcium. Geochim Cosmochim Acta 66:745-758.

Håkanson L, Jansson M. 2002. Principles of lake sedimentology. The Blackburn Press, Caldwell, NJ USA

Hjieltjes AH, Lijklema L. 1980. Fractionation of inorganic phosphorus in calcareous sediments. J Environ Qua. 8: 130-132.

Hupfer M, Gächter R., Giovanoli R. 1995. Transformation of phosphorus species in settling seston and during early sediment diagenesis. Aquat Sci 57:305-324.

Huser BJ. 2012. Variability in phosphorus binding by aluminum in alum treated lakes explained by lake morphology and aluminum dose. Wat Res 46:4697-4704.

Huser BJ, Egemose S, Harper H, Hupfer M, Jensen H, Pilgrim KM, Reitzel K, Rydin E, Futter M. 2016. Longevity and effectiveness of aluminum addition to reduce sediment phosphorus release and restore lake water quality. Wat Res 97:122-132.

Idso SB. 1973. On the concept of lake stability. Limnol Oceanogr 18:681-683.

Istvanovics V, Pettersson K, Rodrigo MA, Pierson D, Padisak J, Colom W. 1993. *Gloeotrichia echinulata*, a colonial cyanobacterium with a unique phosphorus uptake and life strategy. J Plankton Res. 15:531–552.

Istvanovics V, Shafik HM, Presing M, Juhos S. 2000. Growth and phosphate uptake kinetics of the cyanobacterium, *Cylindrospermopsis raciborskii* (Cyanophyceae) in throughflow cultures. Freshwater Biol 43:257–275.

James, W.F., W.D. Taylor, and J.W. Barko. 1992. Production and vertical migration of *Ceratium hirundinella* in relation to phosphorus availability in Eau Galle Reservoir. Canadian Journal of Fisheries and Aquatic Sciences 49:694-700.
James WF, Sorge PW, Garrison PJ. 2015 Managing internal phosphorus loading in a weakly stratified eutrophic lake. Lake Reserv Manage 31:292-305.

James W.F., and J.W. Bischoff. 2015. Relationships between redox-sensitive phosphorus concentrations in sediment and the aluminum:phosphorus binding ratio. Lake Reserv Manage 31:339-346.

James WF. 2017a. Diffusive phosphorus fluxes in relation to the sediment phosphorus profile in Big Traverse Bay, Lake of the Woods. Lake Reserv Manage 33:360-368.

James WF. 2017b. Phosphorus binding dynamics in the aluminum floc layer of Half Moon Lake, Wisconsin. Lake Reserv Manage 33: 130-142.

Jensen HS, Reitzel K, Egemose S. 2015. Evaluation of aluminum treatment efficiency on water quality and internal phosphorus cycling in six Danish lakes. Hydrobiologia 751:189-199.

Kleeberg A. 1997. Interactions between benthic phosphorus release and sulfur cycling in Lake Scharmützelsee (Germany). Wat Air Soil Pollut 99:391-399.

Kleeburg A, Köhler A, Hupfer M. 2012. How effectively does a single or continuous iron supply affect the phosphorus budget of aerated lakes. J Soil Sediments 12:1593-1603.

Kleeburg A, Herzog C, Hupfer M. 2013. Redox sensitivity of iron in phosphorus binding does not impede lake restoration. Water Res 47:1491-1502.

Lalonde K, Mucci A, Quellet A, Gélinas Y, 2012. Preservation of organic matter in sediments promoted by iron. Nature 483:198-200.

Lewandowski J, Schauser I, Hupfer M. 2003. Long term effects of phosphorus precipitations with alum in hypereutrophic Lake Süsser See (Germany). Wat Res 37:3194-3204.

Mortimer CH. 1971. Chemical exchanges between sediments and water in the Great Lakes – Speculations on probable regulatory mechanisms. Limnol. Oceanogr 16:387-404.

Nürnberg GK. 1988. Prediction of phosphorus release rates from total and reductant-soluble phosphorus in anoxic lake sediments. Can J Fish Aquat Sci 45:453-462.

Nürnberg GK. 1995. Quantifying anoxia in lakes. Limnol Oceanogr 40:1100-1111.

Nürnberg GK. 2009. Assessing internal phosphorus load – Problems to be solved. Lake Reserv Manage 25:419-432.

Perakis SS, Welch EB, Jacoby JM. 1996. Sediment-to-water blue green algal recruitment in response to alum and environmental factors. Hydrobiologia 318:165–177.

Pettersson K, Herlitz E, Istvanovics V. 1993. The role of *Gloeotrichia echinulata* in the transfer of phosphorus from sediments to water in Lake Erken. Hydrobiologia 253: 123–129.

Psenner R, Puckso R. 1988. Phosphorus fractionation: Advantages and limits of the method for the study of sediment P origins and interactions. Arch Hydrobiol Biel Erg Limnol 30:43-59.

Rydin E, Malmaeus JM, Karlsson OM, Jonsson P. 2011. Phosphorus release from coastal Baltic Sea sediments as estimated from sediment profiles. Est Coast Shelf Sci. 92: 111–117.

Taylor, W.D., J.W. Barko, and W.F. James. 1988. Contrasting diel patterns of vertical migration in the dinoflagellate *Ceratium hirundinella* in relation to phosphorus supply in a north-temperate reservoir. Canadian Journal of Fisheries and Aquatic Sciences 45:1093-1098.

Vallentyne JR. 1957. Principles of modern limnology. Amer Sci 45:218-244.

Walker WW. 1996. Simplified procedures for eutrophication assessment and prediction: User manual. Instruction Report W-96-2, September 1996, U.S. Army Engineer Waterways Experiment Station, Vicksburg, Mississippi, USA.

Fig. 1. Bathymetric map of North Pipe Lake showing sampling stations

Sediment – upper 5 cm section

Sediment – Vertical profile and diffusive P flux

Water chemistry and thermistors

North Pipe Lake

N
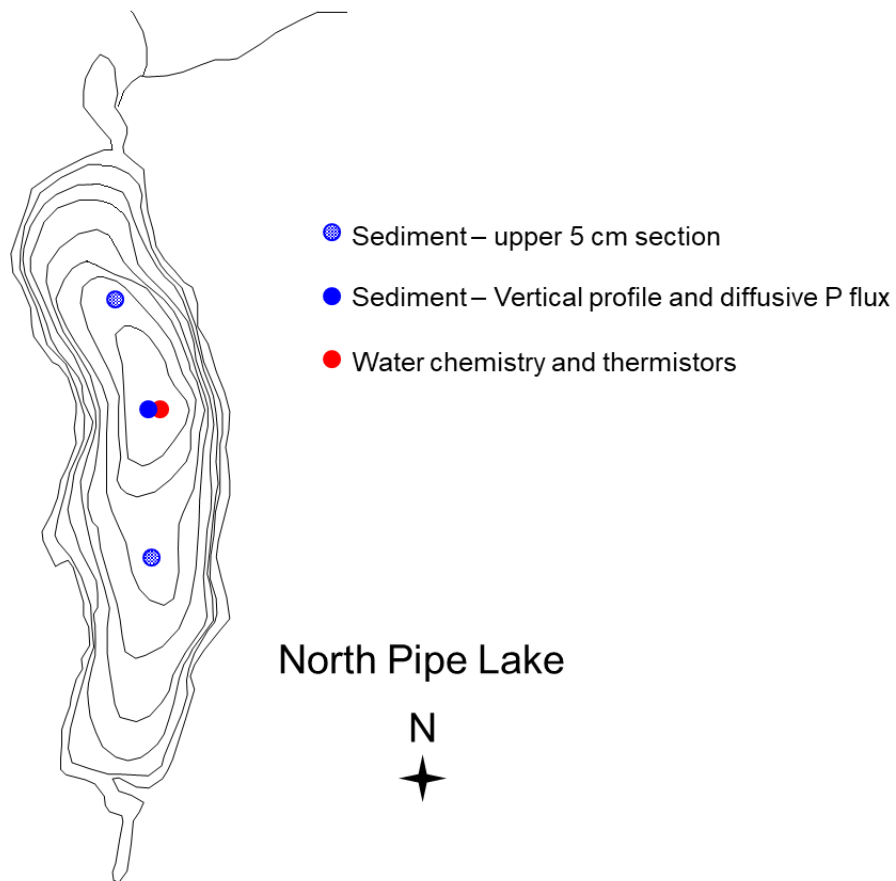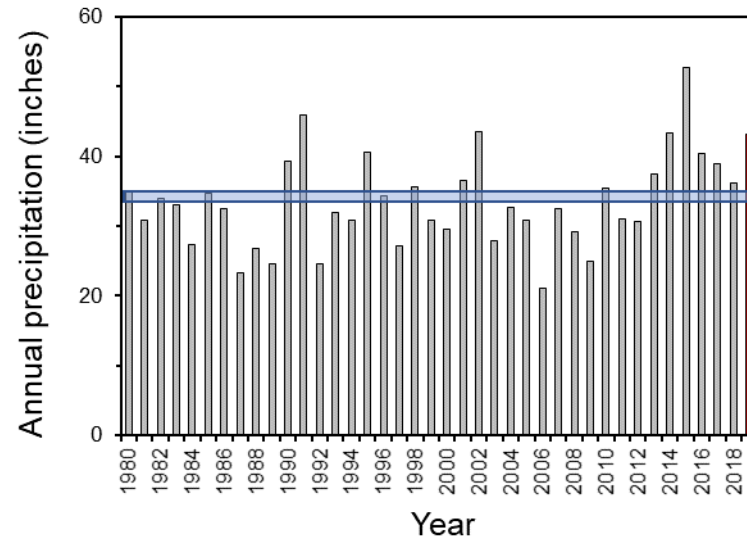
Fig. 2. Variations in annual precipitation measured at Amery Wisconsin. Red bar represents 2019. Horizontal blue line denotes average precipitation since 1980.
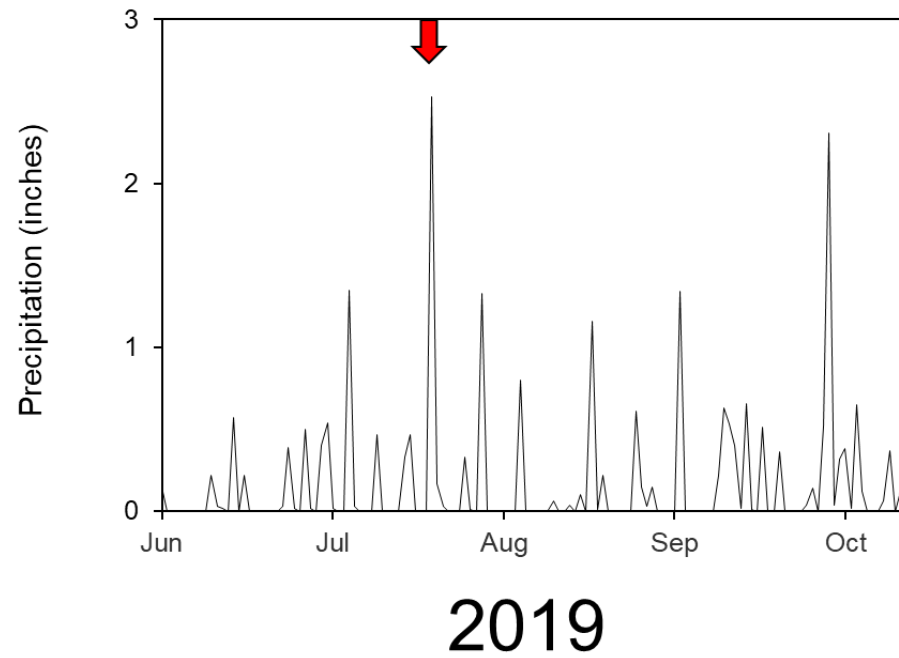
Fig. 3. Seasonal variations in daily precipitation measured at Amery WI. Red arrow denotes the time of tornados and severe storms in the area (19 July).
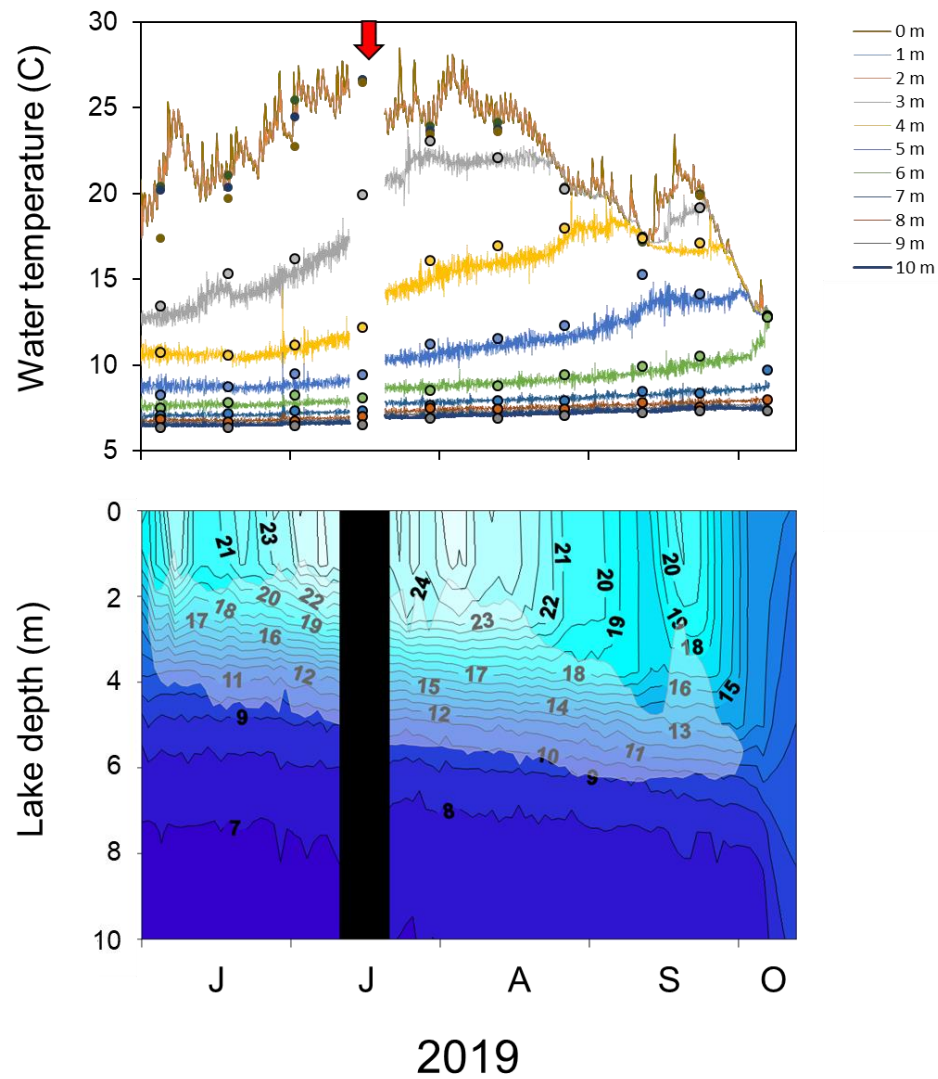
Fig. 4. Seasonal variations in hourly water temperature measured at 1-m depth intervals (upper panel) and temperature contours (lower panel) at the sampling station located in North Pipe Lake 2019. Red arrow denotes the time of tornados and severe storms in the area (19 July).

31
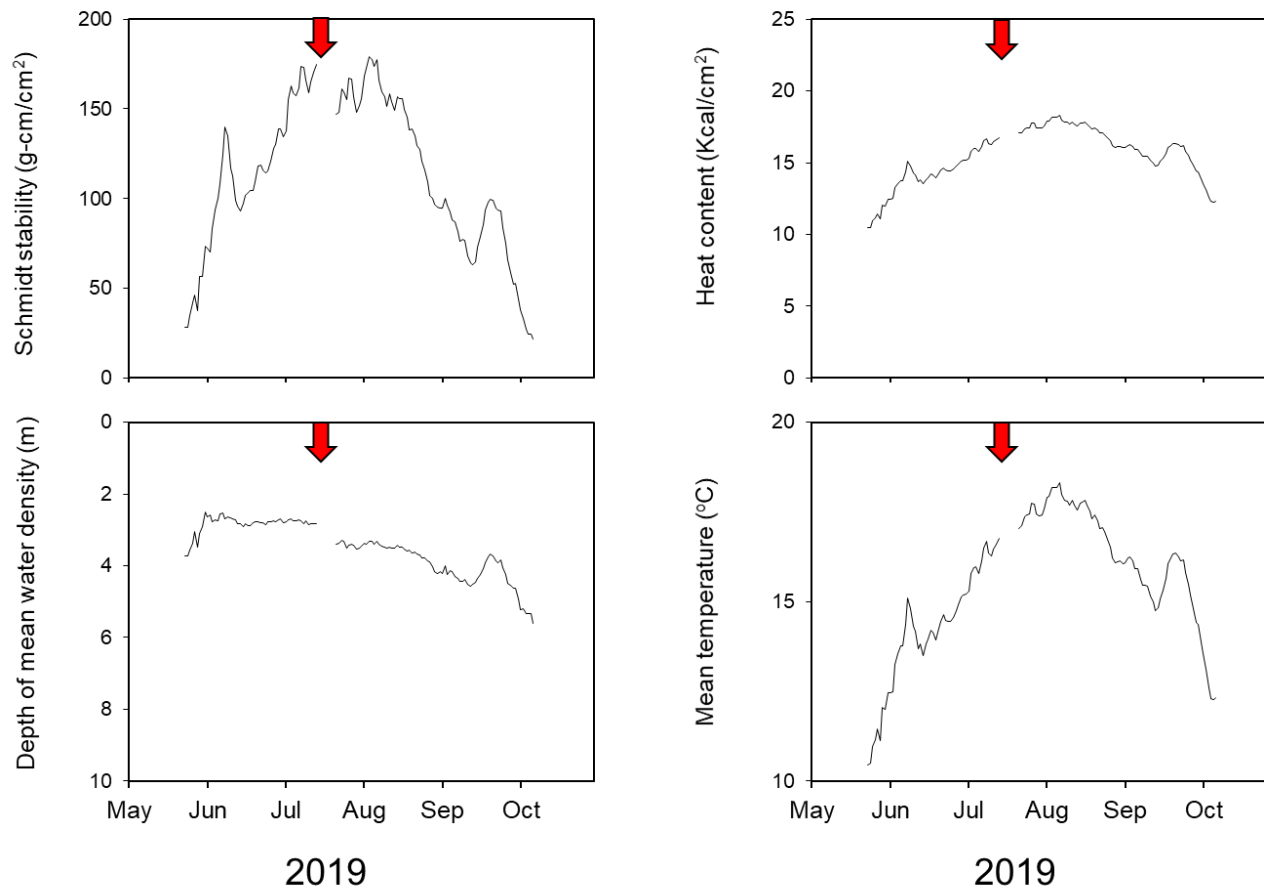
Fig. 5. Seasonal variations in Schmidt stability, depth of mean water density (i.e., ~ location of the thermocline), lake heat content, and lake mean temperature in North Pipe Lake 2019. Red arrow denotes the time of tornados and severe storms in the area (19 July).
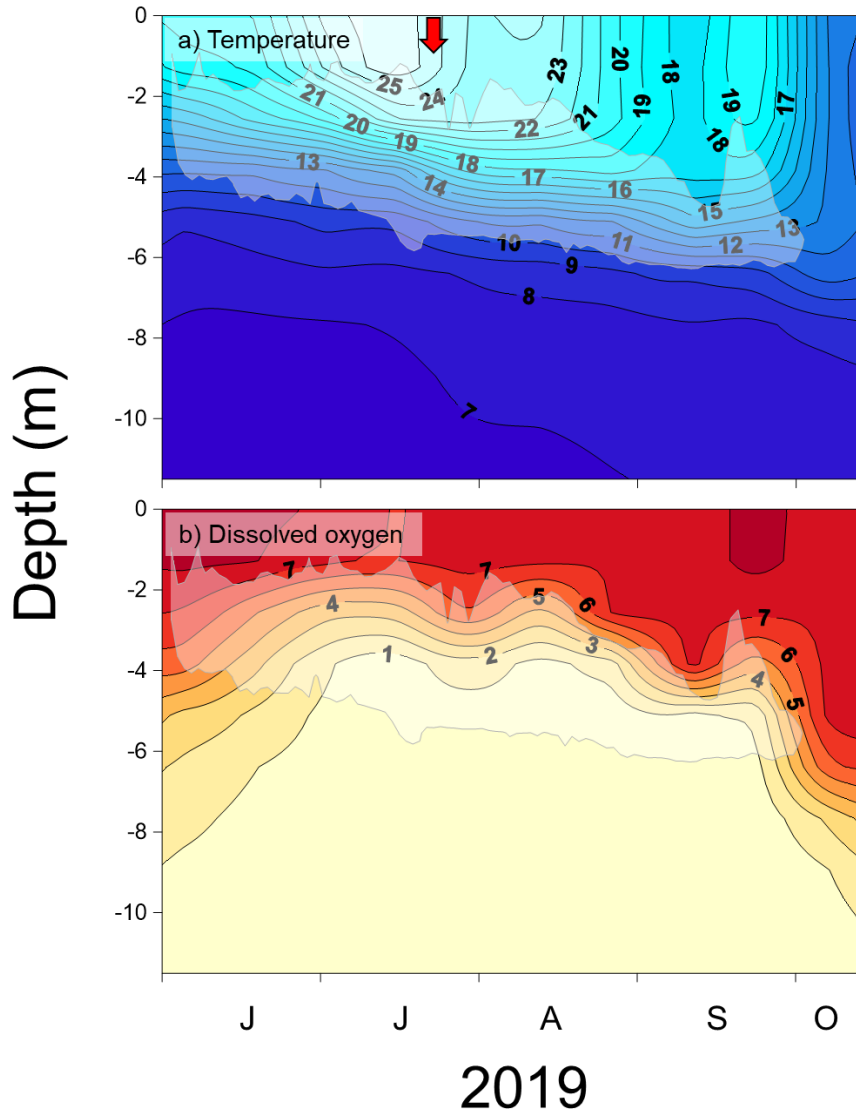
Fig. 6. Seasonal and vertical variations in water temperature (upper panel) and dissolved oxygen (lower panel) from routine biweekly in situ monitoring information collected at the North Pipe Lake sampling station in 2019. Red arrow denotes the time of tornados and severe storms in the area (19 July). The white shaded areas represent the approximate location of the metalimnion (Relative Thermal Resistance to Mixing = 30, Vallentyne 1957).

Fig. 7. Seasonal variations in bottom (i.e., ~ 0.25 m above the sediment surface) total and soluble iron and phosphorus. Red arrow denotes the time of tornados and severe storms in the area (19 July).
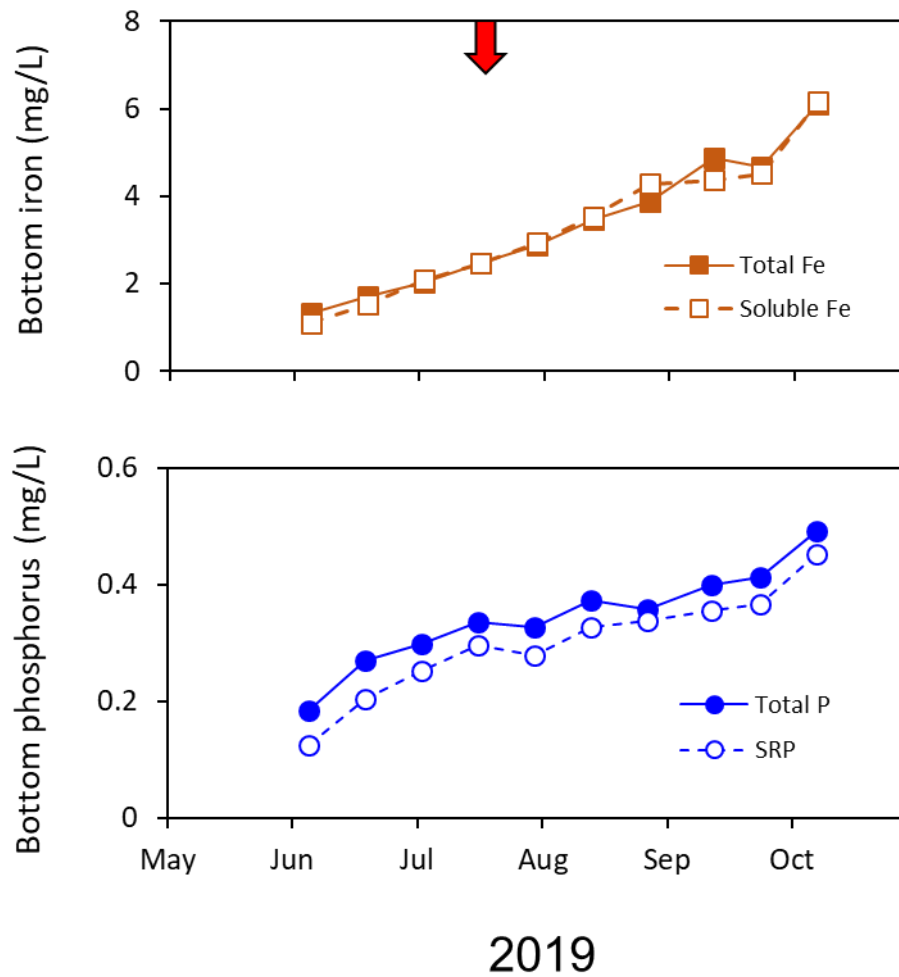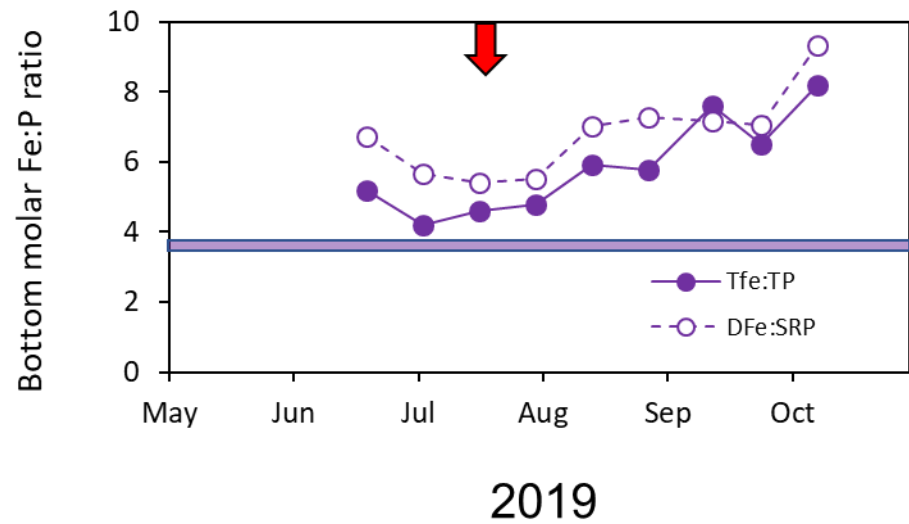
Fig. 8. Seasonal variations in the total Fe: total P (TFe:TP) ratio and the dissolved Fe:soluble reactive P (DFe:SRP) ratio of bottom samples collected in North Pipe Lake 2019. Red arrow denotes the time of tornados and severe storms in the area (19 July).

Fig. 9. Seasonal and vertical variations in total phosphorus (P), soluble reactive P, and chlorophyll in North Pipe Lake 2019. Red arrow denotes the time of tornados and severe storms in the area (19 July). The white shaded areas represent the approximate location of the metalimnion (Relative Thermal Resistance to Mixing = 30, Vallentyne 1957).
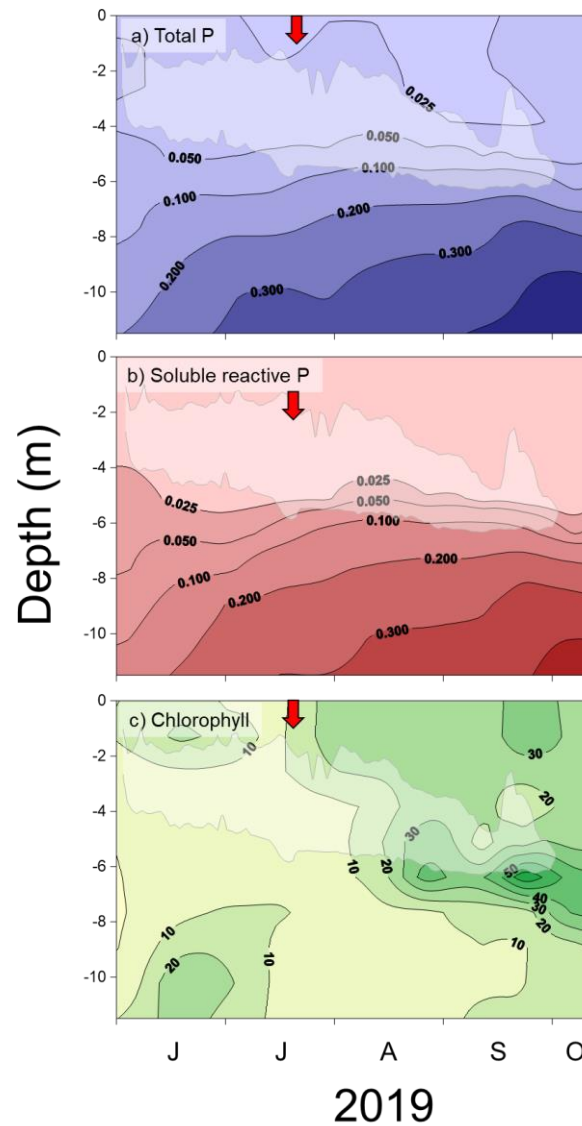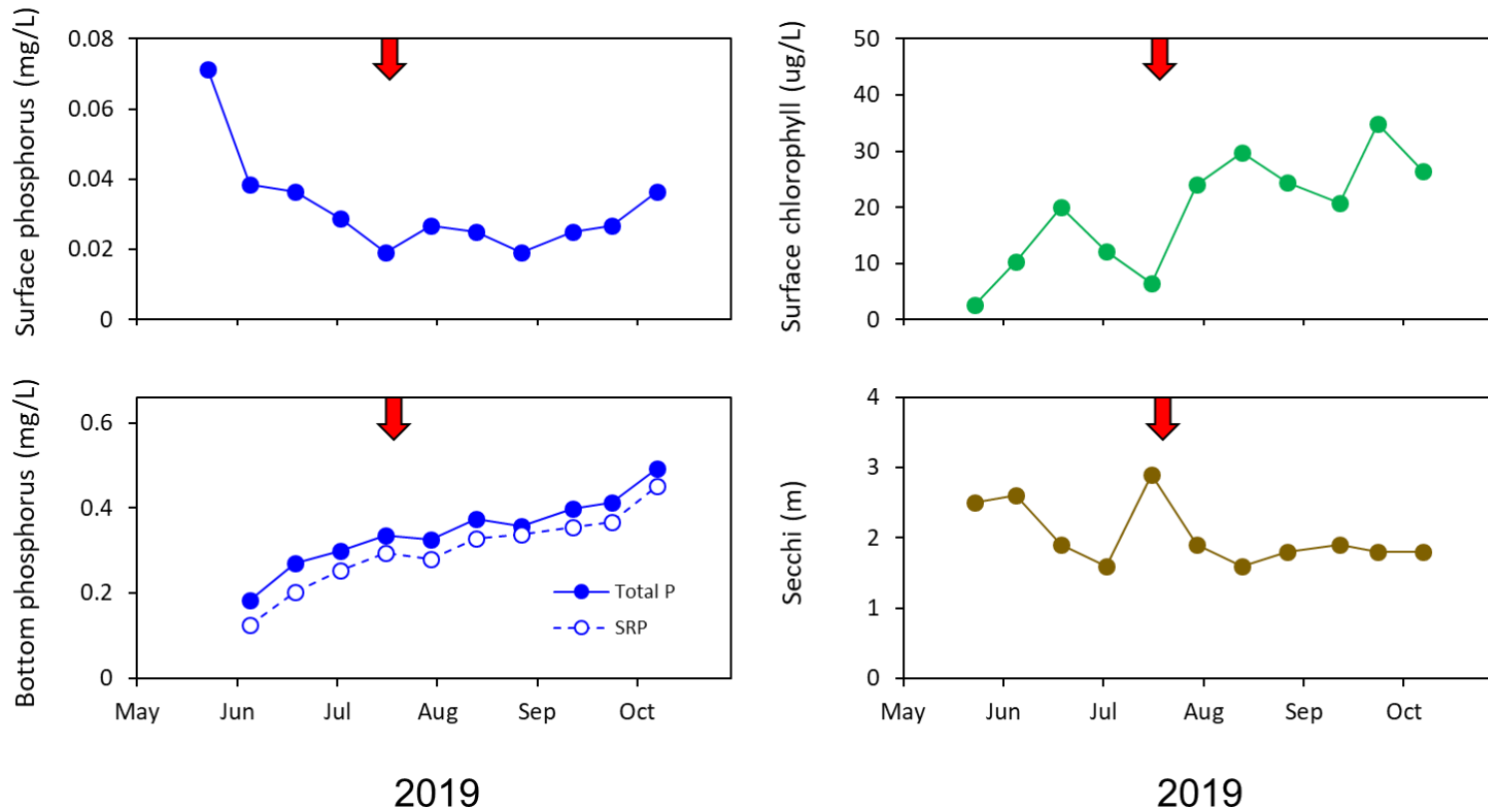
Fig. 10. Seasonal variations in total phosphorus (P) in the upper 2-m water column (upper left), and total P and soluble reactive P (SRP) concentrations in the hypolimnion above the sediment (lower left), chlorophyll (2-m integrated sample, upper right), and Secchi transparency (lower right) in North Pipe Lake 2019. Red arrow denotes the time of tornados and severe storms in the area (19 July).
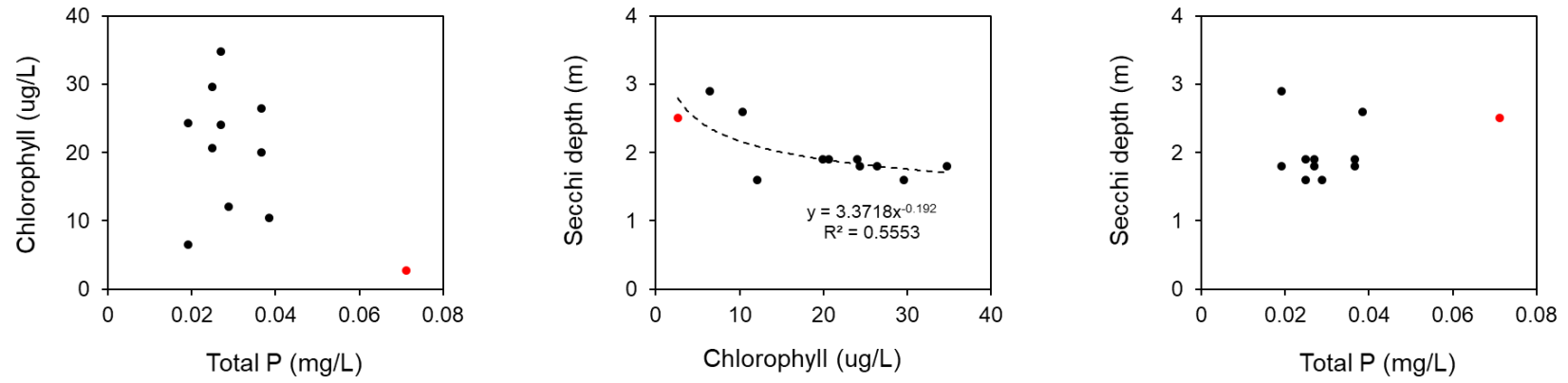
Fig. 11. Relationships between limnological trophic state variables. Red dot represents the water sample collected in late May 2019.
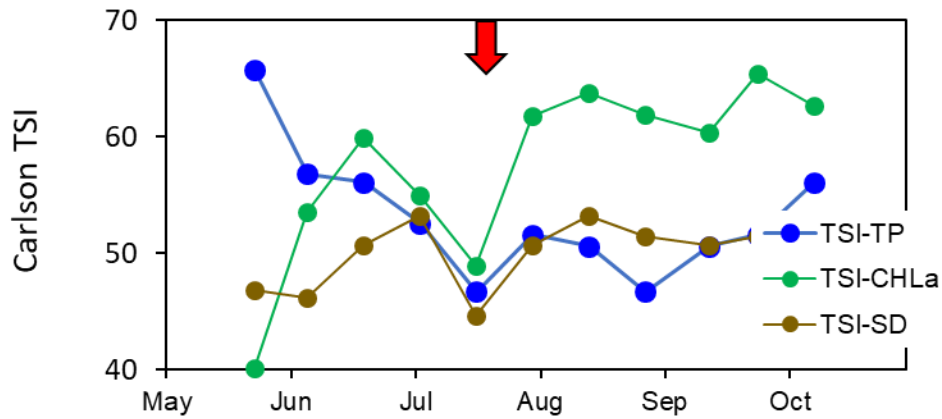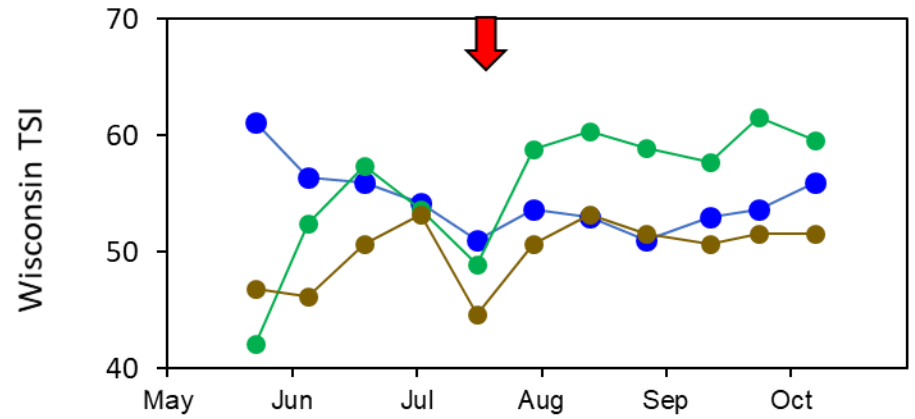
Fig. 12. Seasonal variation in Carlson and Wisconsin Trophic State Index values for North Pipe Lake 2019. Red arrow denotes the time of tornados and severe storms in the area (19 July).

Fig. 13. Seasonal variations in the chlorophyll:total phosphorus (CHLa:TP) ratio in North Pipe Lake 2019. Red arrow denotes the time of tornados and severe storms in the area (19 July).

Fig. 14. Changes in soluble reactive phosphorus mass and concentration versus days of incubation in replicate sediment core incubation systems subjected to anaerobic conditions.

The figure shows two panels with "Phosphorus in the overlying water column" as the vertical axis label. The top panel plots Mass (mg) from 0 to 0.2, annotated with "4.03 mg/m² d (± 0.58 SE) @ 10 °C". The bottom panel plots Concentration (mg/L) from 0 to 0.5. Both panels share the horizontal axis "Days of incubation" from 0 to 10.
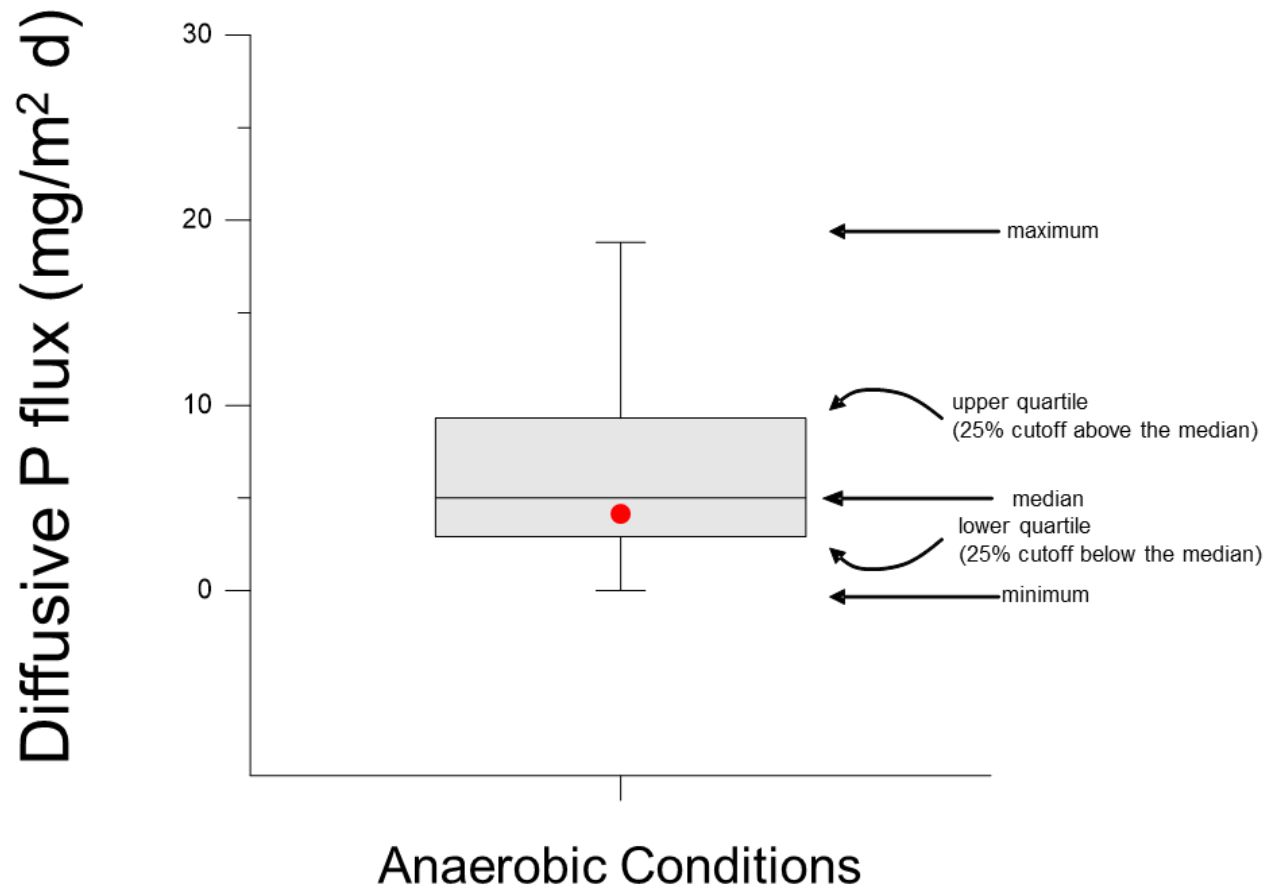
Fig. 15. Box and whisker plot comparing laboratory-derived diffusive P flux from sediment collected in North Pipe Lake (red circle) with other lake sediments in the region.
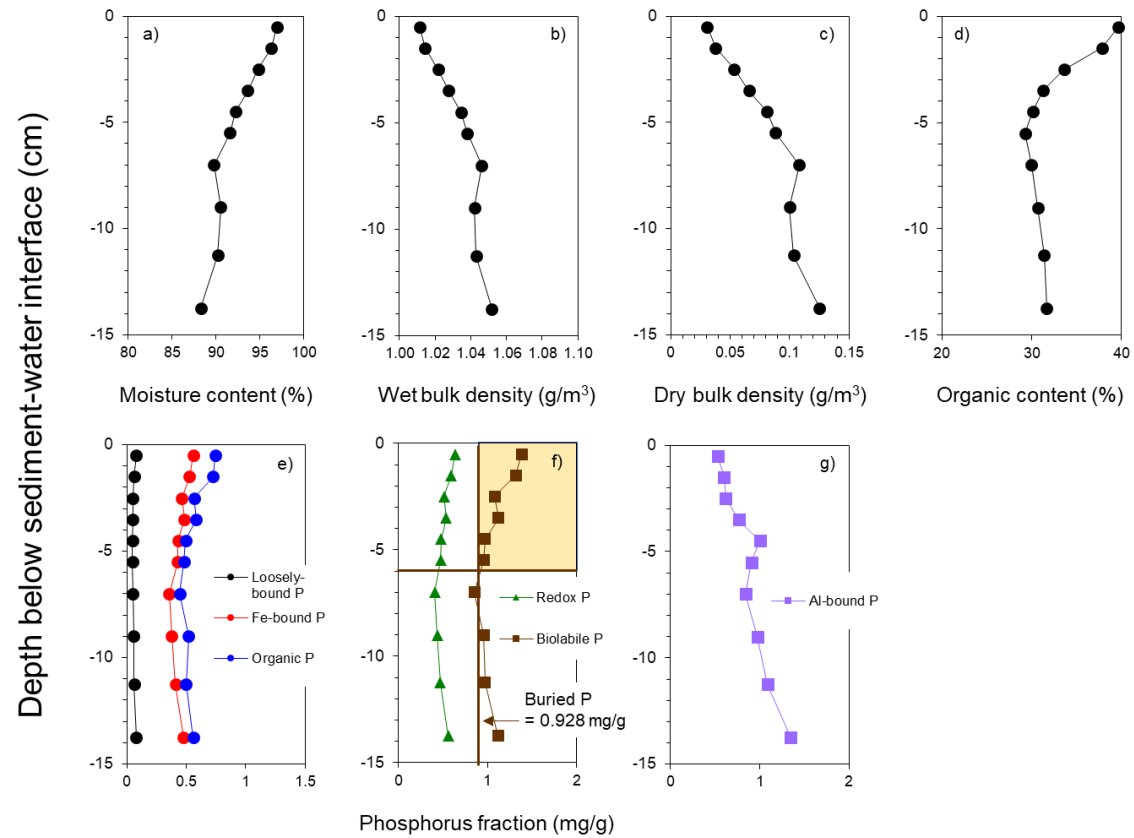
Fig.16. Central station sediment core vertical profiles of physical-textural characteristics and phosphorus fractions. The yellow shaded area denotes the sediment redox P concentrations used to estimate alum dose.
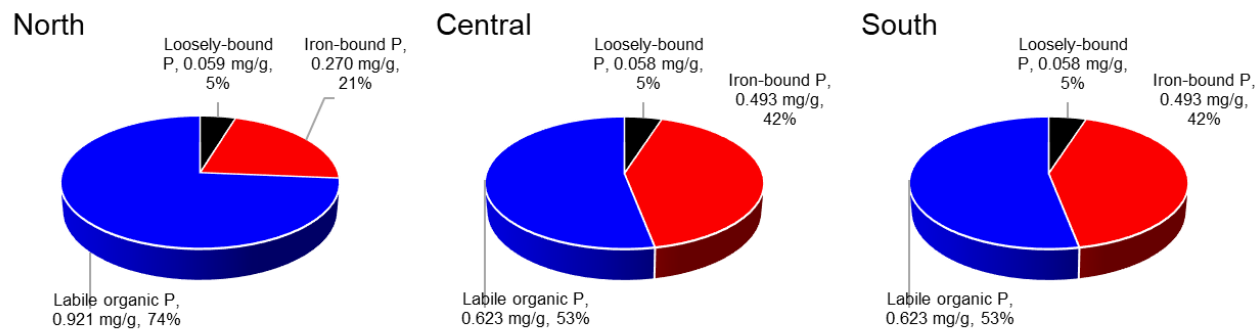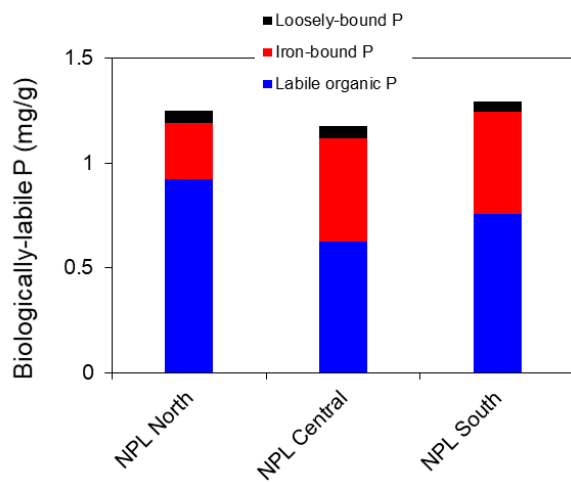
Fig. 17. Percent composition of the biologically-labile phosphorus fraction in the upper 5-cm of sediment collected at the north, central, and south stations in North Pipe Lake 2019.

Fig. 18. Box and whisker plot comparing concentrations of loosely-bound, iron-bound, and labile organic phosphorus (P) from the upper 5-cm sediment layer in North Pipe Lake with other lake sediment concentrations in the region.
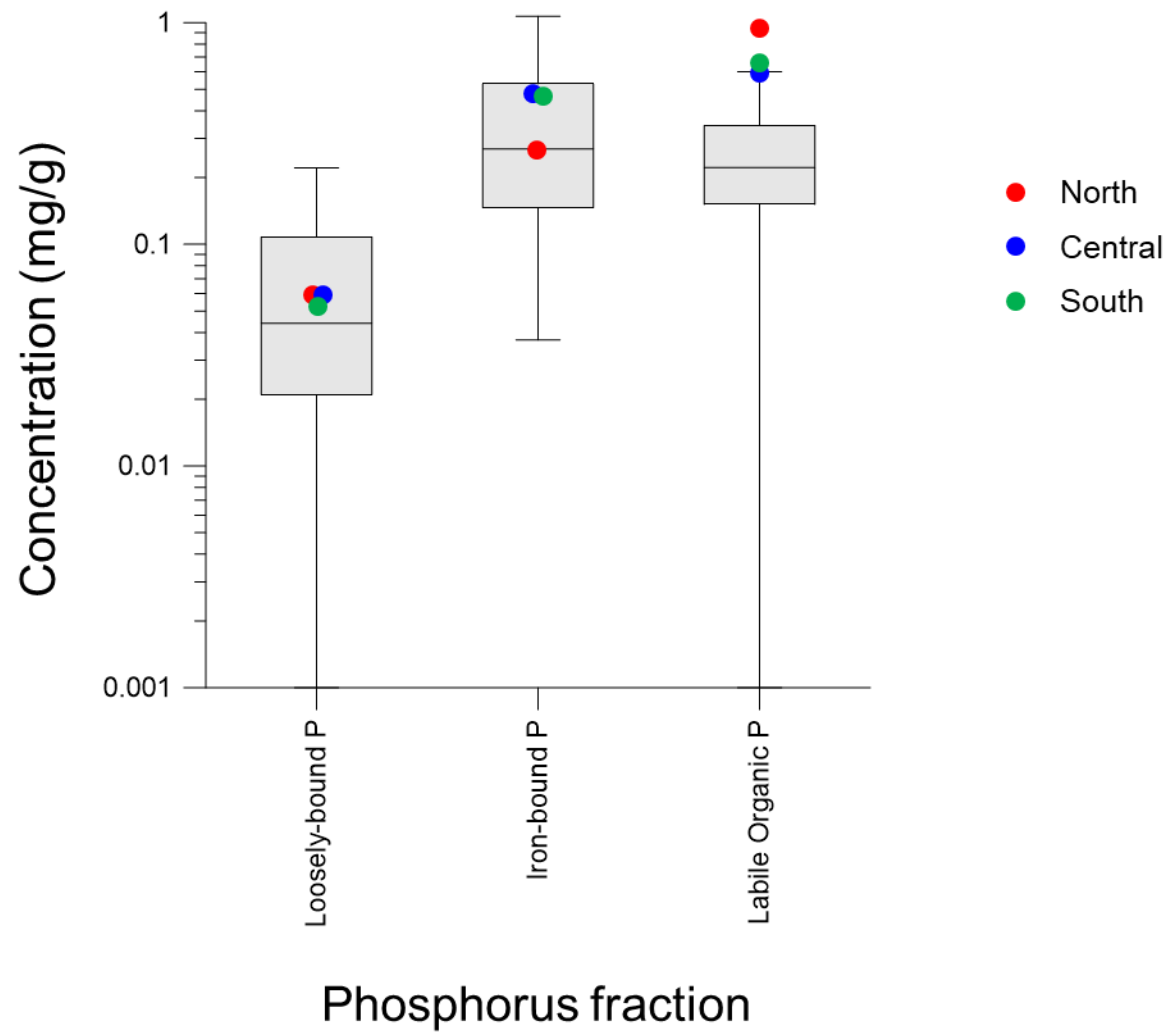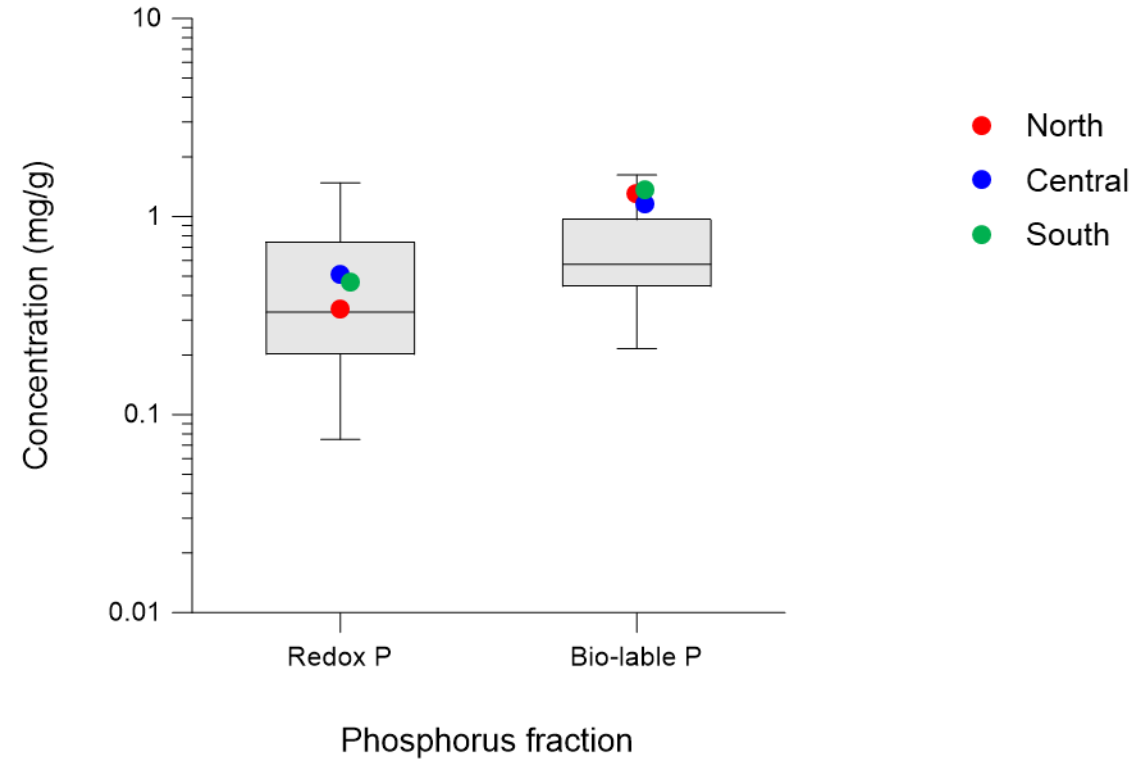
Fig. 19. Box and whisker plot comparing concentrations of redox phosphorus (P) and biologically-labile P from the upper 5-cm sediment layer in North Pipe Lake with other lake sediment concentrations in the region.
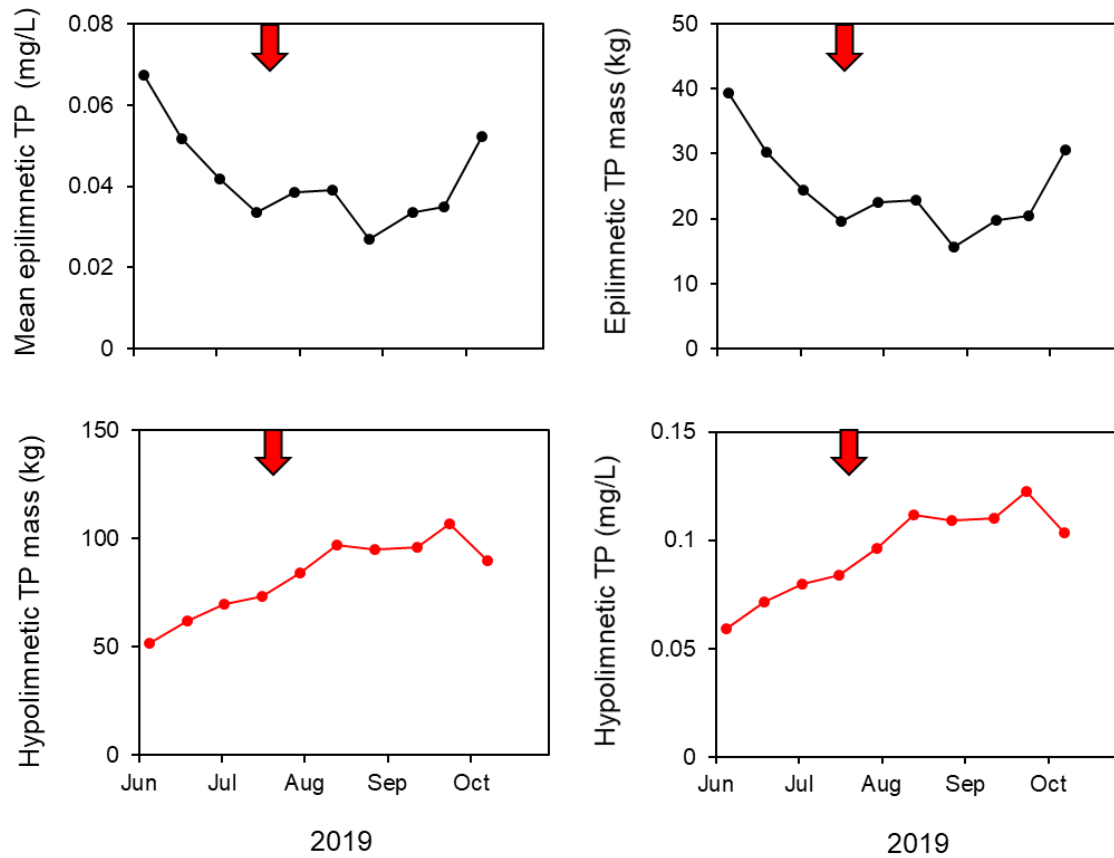
Fig. 20. Seasonal variations in epilimnetic (depth <= 3 m) and hypolimnetric (depth > 3 m) total P (TP) mass and concentration in 2019. Red arrow denotes the time of tornados and severe storms in the area (19 July).